Surfaceemitting secondharmonic generator for waveguide study

D. Vakhshoori, M. C. Wu, and S. Wang

Citation: Applied Physics Letters **52**, 422 (1988); doi: 10.1063/1.99430
View online: http://dx.doi.org/10.1063/1.99430
View Table of Contents: http://scitation.aip.org/content/aip/journal/apl/52/6?ver=pdfcov
Published by the AIP Publishing

Surface-emitting second-harmonic generator for waveguide study

D. Vakhshoori, M. C. Wu, and S. Wang
Department of Electrical Engineering and Computer Sciences, and the Electronics Research Laboratory, University of California, Berkeley, California 94720

(Received 25 August 1987; accepted for publication 1 December 1987)

A novel surface emission of coherently generated second-harmonic wave is reported for the first time. The technique is used for the observation of the difference in propagation constant of the TE_0 and TM_0 mode of GaAs/AlGaAs waveguide cavity to a high degree of accuracy. In this technique the second-harmonic signal propagates out from the top surface of the waveguide structure, converting the modal phase difference between TE_0 and TM_0 modes into intensity variation along the waveguide length. The second-harmonic signal is easily observable by the naked eye, and the technique does not require wavelength tuning or mechanical movement for the measurement of birefringence.

In this letter we report phase-matched, coherent, second-harmonic generation of a mode-locked Nd:YAG laser beam propagating pependicular to the direction of flow of the fundamental beam. In conventional second-harmonic-generation techniques, the amount of second harmonic propagating out perpendicular to the direction of a forward propagating fundamental beam is negligible, since the phase-matching condition is violated. However, in the technique presented here, a standing wave of second-harmonic polarization is generated along the waveguide cavity. The second-harmonic signal generated this way is show to be coherent and to satisfy the wave vector conservation. To the best of the authors' knowledge, this is the first time the second-harmonic wave has been generated in this manner and used to study waveguide parameters.

The parameter studied in this experiment is the modal birefringence of a waveguide structure. The difference in propagation constants of the TE_0 and TM_0 mode of a GaAs/AlGaAs waveguide is of paramount importance for an efficient electro-optic waveguide TE↔TM mode conversion[1] and wavelength filtering.[2] Waveguide polarization conversion is a basic signal processing function and will be useful in realizing single-mode communication systems. In addition to its integrability, the TE↔TM mode convertor together with integrated polarizer[3] can be used as a high-speed optical modulator. TE↔TM mode convertor can be realized as a broad-band or narrow-band (full width at half-maximum ~ 4.5 Å)[2] polarization convertor. Thus TE↔TM convertors can be used as a polarization convertor, an optical modulator, or a wavelength filter in future opto-electronic circuits. However, to realize any of the above devices, an exact knowledge of modal phase difference $\Delta\beta = \beta_{TE} - \beta_{TM}$ is required. The observation of surface emission of the second-harmonic signal gives the modal phase difference accurately (error $\lesssim 1\%$), directly, and without any ambiguity. Furthermore, the requirement that the second-harmonic signal is not absorbed strongly by the top cladding layer of the waveguide is not severe, since some sommon electro-optic polarization modulators on GaAs are made with transparent top cladding layer.[1]

The experimental setup used is shown in Fig. 1. Abut 20 mW average power from a mode-locked Nd:YAG ($\lambda = 1.064\ \mu$m) laser output with a repetition rate of 82 MHz and pulse width of 100 ps was focused by a 40× objective lens on a facet of a waveguide cavity 1 mm long. The waveguide structure is shown in the inset of Fig. 1. The output power from the other facet was measured to be ~ 1 mW. The second-harmonic generation was monitored by looking into a low-magnification microscope and optimized by changing the polarization of the incident fundamental beam by using a half-wave plate to equalize the power coupled into TE_0 and TM_0 mode of the waveguide. Once the green light (532 nm) was optimized by eye, the image of the near field was recorded on a 1600 ASA Fuji film exposed for 3 min. The picture was taken by using a commercial camera and looking into the eye piece of the microscope. The picture is shown in Fig. 2. There are 16 periods of intensity modulation in 1 mm corresponding to $\beta_{TE_0} - \beta_{TM_0} = 50$ rad/mm. This result is obtained by theoretical consideration of the relation between second-harmonic-intensity modulation and modal phase difference.

From theory we have

$$E_i(z) = \mathrm{Re}\left[e^{i\omega t}(A_i e^{-\gamma_i z} + B_i e^{\gamma_i (z-2L)})\right],$$
$$A_i = \frac{E_{0i} t_i}{1 - r_i^2 e^{-2\gamma_i L}}, \quad \frac{B_i}{A_i} = r_i, \tag{1}$$

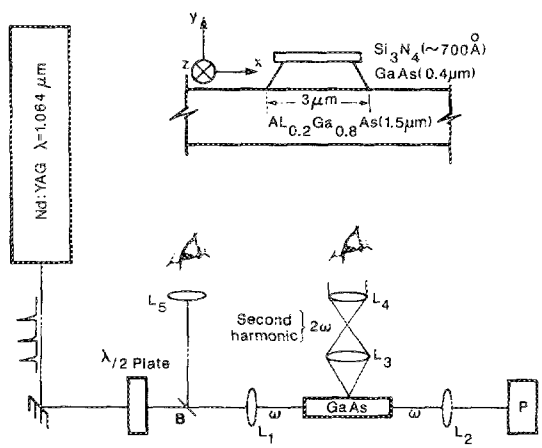

FIG. 1. Experimental setup used. L_1 couples light into the GaAs waveguide. L_2 collimates the light to the power meter P. L_3 and L_4 form a low-magnification microscope. L_5 and beam splitter B are used to adjust coupling through lens L_1 to the waveguide. The $\lambda/2$ plate is used to change the polarization of the incident fundamental beam. The waveguide under consideration is shown in the inset. It was grown by molecular beam epitaxy over [100] oriented GaAs wafer.

 0003-6951/88/060422-03$01.00

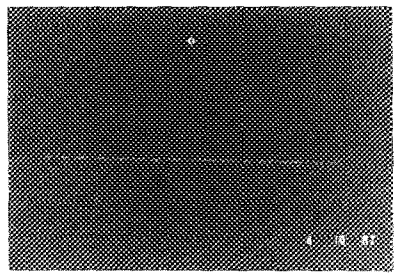

FIG. 2. Picture of the square of the near-field pattern of the second harmonic of Nd:YAG generated across the waveguide. There are 16 periods of variation over 1 mm of waveguide length, giving a period of $\Lambda \sim 63\ \mu m$.

where $i = x$ and y corresponds to the E_x and E_y component of TE_0 and TM_0 modes, respectively (z is the direction of propagation along the waveguide), E_{0i} is the incident electric field on the input facet of the waveguide, t_i and r_i are transmission and reflection coefficients, and $\gamma_i = \alpha_i + i\beta_i$ is the complex propagation constant. The wafer under consideration has [100] surface orientation. This fact combined with the symmetry of the nonlinear susceptibility tensor $\hat{\chi}^{(2)}$ of GaAs yields second-harmonic polarization of the form $\mathbf{p}^{(2\omega)} \propto (2E_x E_y \hat{x} + E_x^2 \hat{y})$. The first component of polarization is along the polarization of TE_0, and the second term is polarized like the TM_0 mode. The TM_0-like component of second-harmonic polarization has y-directed polarization and hence cannot contribute to the radiation of second harmonic coming out of the top surface of the waveguide. However, the TE_0-like polarization of the second harmonic can radiate out of the top surface. If we keep only the sum frequency term and using Eq. (1), we obtain

$$\begin{aligned} p^{(2\omega)} &\propto \mathrm{Re}(E_1 E_2) \\ &= \mathrm{Re}[e^{2i\omega t}(A_1 A_2 e^{-2\bar{\gamma}z} + B_1 B_2 e^{+2\bar{\gamma}(z-2L)})] \\ &\quad + \mathrm{Re}\left[e^{2i\omega t}(A_1 B_2 e^{-2\bar{\gamma}L}) \times \left(e^{-\Delta\gamma(z-L)} + \frac{B_1 A_2}{A_1 B_2} e^{\Delta\gamma(z-L)}\right)\right], \end{aligned} \tag{2}$$

where $\bar{\gamma} = \frac{1}{2}(\gamma_1 + \gamma_2) = \bar{\alpha} + i\bar{\beta}$, $\Delta\gamma = \gamma_1 - \gamma_2 = \Delta\alpha + i\Delta\beta$. The term of the form $e^{2i(\omega t \pm \bar{\gamma}z)}$ cannot radiate perpendicular to z direction and will be ignored. Also from Eq. (1), $B_1 A_2 / A_1 B_2 = r_1/r_2$. Using this in Eq. (2), we obtain

$$p^{(2\omega)} \sim \mathrm{Re}\left[e^{2i\omega t}(A_1 B_2 e^{-2\bar{\gamma}L})\left(e^{-\Delta\gamma(z-L)} + \frac{r_1}{r_2} e^{\Delta\gamma(z-L)}\right)\right]. \tag{3}$$

The time-averaged second-harmonic radiation is then

$$\begin{aligned} \langle P^{(2\omega)} \rangle_t &\propto (p^{(2\omega)} p^{*(2\omega)}) \\ &\propto |A_1 B_2|^2 e^{-4\bar{\alpha}L} \times \left[\frac{1}{2}\left(a + \frac{1}{a}\right) + \cos[2\Delta\beta(z-L)]\right], \end{aligned} \tag{4}$$

where $a = (r_1/r_2)e^{2\Delta\alpha(z-L)} = 1 - \Delta a$. In terms of Δa, Eq. (4) reduces to

$$\langle P^{(2\omega)} \rangle_t \propto |A_1 B_2|^2 e^{-4\bar{\alpha}L}\left(1 + \frac{(\Delta a)^2}{2} + \frac{O(\Delta a)^3}{2} + \cos[2\Delta\beta(z-L)]\right). \tag{5}$$

For low-loss birefringence ($|2\Delta\alpha L| = 2|\alpha_1 - \alpha_2|L \ll 1$), Δa becomes $1 - r_1/r_2$, which is less than 0.2 for usual waveguides.[4] Therefore, we can safely ignore Δa in Eq. (5). Figure 3 shows the theoretical variation of $\langle P^{(2\omega)} \rangle_t$ as a function of length across the waveguide. For the purpose of calculation, the actual waveguide is approximated by a slab waveguide shown in the inset of Fig. 3. As can be seen, the theory agrees well with the experimentally observed second-harmonic variation of Fig. 2. The most uncertain parameter of the waveguide is the aluminum mole fraction of the cladding layer, which was approximately 20%. Then according to Eq. (5), the birefringence at $\lambda = 1.0642\ \mu m$ is given by

$$\Delta\beta = \beta_{TE_0} - \beta_{TM_0} = \pi/\Lambda = 50\ \mathrm{rad/mm}, \tag{6}$$

where $\Lambda \simeq 63\ \mu m$ is the period of the variation of the second harmonic signal observed. The experimentally observed $\Lambda \simeq 63\ \mu m$ agrees well with the theoretical prediction of $\Lambda \sim 60\ \mu m$ (Fig. 3). There are several points that need further discussion. For small Δa (that is $r_1/r_2 \simeq 1$), the second-harmonic polarization has a standing-wave profile, varying sinusoidally in z along the direction of the waveguide. This standing-wave polarization acts as a source for the radiation of second-harmonic signal. Assuming that the waveguide is charge free, the polarization profile generates an electric field along its direction, $\mathbf{E} = -4\pi\mathbf{P}$. Since the lens of the camera in our experiment maps the near-field pattern of the electric field across the waveguide to the image plane on the film negative, the resulting picture of Fig. 2 registers the time-averaged square of the near-field pattern or the time-averaged square of polarization profile across the waveguide. This point shows the relation of Eq. (5) to Fig. 2.

Another point to consider is the coherence of the second harmonic signal (SHS). The far-field pattern is approximately proportional to the Fourier transform of the near-field pattern. With the use of the near-field pattern discussed above, the far-field pattern is calculated to have intensity peaks at angles $|\theta| = \lambda_{2\omega}/2\Lambda \ll 1$ rad, where the angle is measured in the y-z plane (Fig. 1) with the y axis referring to $\theta = 0$. This prediction of the theory can account for the fact that when the lenses L_3 and L_4 in Fig. 1 were tilted from the direction perpendicular to the sample surface in the y-z plane, the intensity of SHS would sharply decrease. This observation confirms the coherent nature of the second-harmonic signal.

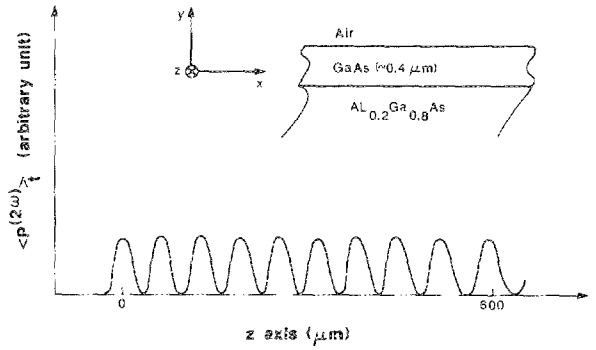

FIG. 3. Theoretical variation of $\langle P^{(2\omega)} \rangle_t$ along the waveguide length. The actual waveguide is approximated by an equivalent slab waveguide shown in the inset of the figure. For the parameters used, we obtain $\Lambda \sim 60\ \mu m$.

The third point to consider is the phase-matching condition. A standing wave can be decomposed into a forward and a backward propagating wave with wave vector K and $-K$. Therefore, the net wave vector of the standing wave is zero. Furthermore, if we express the fundamental electric field profile [Eq. (1)] in terms of a sum of a standing wave and a propagating wave and following the steps leading to Eq. (5), we find that the second-harmonic radiation perpendicular to the waveguide surface is only the result of interaction of the standing-wave component of TE_0 and the standing-wave component of TM_0 modes. Also, the near-field pattern of the SHS is described by a standing wave. This means that the sum of the initial interacting fundamental wave vectors is equal to the sum of the final second-harmonic wave vectors (which equals zero). It should also be noted that since the SHS is not generated collinear to the fundamental beam, the concept of phase matching is not applicable in its conventional sense. For noncollinear second-harmonic generation, the condition for the highest possible efficiency is the conservation of total wave vectors.

In summary, a novel second-harmonic generation technique is theoretically and experimentally analyzed. The second-harmonic signal obeys wave vector conservation, is coherent, and propagates perpendicular to the fundamental beam. This perpendicular propagation makes this technique useful for the study of waveguide parameters. The experiment reported yielded the modal phase birefringence $\Delta\beta = \beta_{TE_0} - \beta_{TM_0}$ accurately, directly, and unambiguously in the GaAs/AlGaAs waveguide structure under consideration. The knowledge of the modal phase birefringence is crucial in design of TE↔TM mode convertors, wavelength filters, and TE↔TM optical modulators. These devices are important part of wavelength multiplexing systems and other future integrated opto-electronics circuits.

This work was supported by Bell Communications Research and the National Science Foundation grant No. ECS-8410838.

[1]F. K. Reinhart, R. A. Logan, and W.R. Sinclair, IEEE J. Quantum Electron. **QE-18**, 763 (1982).
[2]R. C. Alferness, Appl. Phys. Lett. **36**, 513 (1980).
[3]M. Masuda and J. Koyama, Appl. Opt. **16**, 2994 (1977).
[4]T. Ikegami, IEEE J. Quantum Electron. **QE-8**, 470 (1972).